International Journal of Environment and Geoinformatics 11(3):060-068 (2024)

Research Article

Sustainable Biopolymer Composites From Perlite, Plasticized and Unplasticized Poly(Lactic Acid)

Hatice Aylin Karahan Toprakci[1,2*], Deniz Yilmaz Savci[2], Ozan Toprakci[1,2]

[1] Department of Polymer Materials Engineering, Engineering Faculty, Yalova University, Yalova, Türkiye
[2] Institute of Graduate Studies, Yalova University, Yalova, Türkiye

* Corresponding author: H. A. Karahan Toprakci
E-mail: aylin.toprakci@yalova.edu.tr

Received: 12.04.2024
Accepted: 03.09.2024

How to cite: Karahan Toprakci, et al.,(2024). Sustainable Biopolymer Composites From Perlite, Plasticized and Unplasticized Poly(Lactic Acid). *International Journal of Environment and Geoinformatics (IJEGEO)*, 11(3): 060-068. doi. 10.30897/ijegeo.1467716

Abstract

In recent years, ecological pollution has reached critical levels and that has been experienced as climate change by all living organisms. Slowing down the negative effects of climate change depends on changing our consumption behavior. Based on that, people tend to prefer more environmentally friendly, sustainable raw materials, products, and processes. Since polymers are one of the most widely used raw materials in the world, any improvement regarding their recycling or biodegradation process can significantly reduce the damage to nature. Considering this fact, manufacturers are taking initiatives to develop such products in line with the demand from consumers. As is known, poly(lactic acid) (PLA) is one of the most consumed biodegradable polymers in the market; however, there are various problems especially in film production, due to its rigid structure. Plasticization is the easiest route to minimize this disadvantage. The aim of this study is to produce and characterize PLA composites with increased flexibility by using sustainable natural materials. In this context, glycerol-plasticized PLA and unplasticized PLA composites were prepared using perlite, a natural additive, and their morphological, thermal, and mechanical properties were investigated.

Keywords: Poly (lactic acid) (PLA), Perlite, Plasticization, Polymer Composites

Introduction

The world's ecosystem consists of many living and non-living components. These components interact because they are directly or indirectly connected and/or dependent on each other, and the balance of the ecosystem depends on their continuity. The concept of sustainability, which fundamentally arises from the need to ensure the ecosystem's continuity, can be defined as the optimal use of existing resources and opportunities without waste, so as not to disrupt the ecological balance and to pass them on to future generations in sufficient quantity. In this context, the balance of production, consumption, and economy, along with the sustainable transference of natural resources to future generations, should be ensured by considering social equity.

The first step in developing sustainable products within the scope of polymer materials engineering is ensuring the sustainability of the materials. The primary aim of this study is to develop sustainable composite materials. These sustainable materials can be either natural or synthetic, as long as they are made from sustainable raw materials. Poly(lactic acid) (PLA) is one of the most widely used biopolymers in the world, thanks to its ease of production and its ability to be tailored with tunable properties. PLA is used in a wide range of applications, from 3D-printing and injection molding to barrier coatings, as well as fiber and film production. Despite these advantages, PLA is a rigid polymer with low elongation at break and limited flexibility. To enhance the flexibility of PLA, plasticization is the most widely used method in recent years (Al-Mulla et al., 2010; Carpintero et al., 2022; Grigale, 2010; Halász and Csóka, 2013; Kantee and Kajorncheappunngam, 2017; D. Li et al., 2018; Ljungberg and Wesslén, 2005; Martino et al., 2009; Xu and Qu, 2009; YousefniaPasha et al., 2021; Yuan et al., 2016). Plasticization is one of the common techniques in polymer processing used for various purposes, including lowering the glass transition temperature (T_g) of the polymers, making the process easier, increasing the flexibility of the final product. Environmental concerns have led to various requirements and restrictions on materials. From that perspective, plasticizers that are renewable, sustainable, and biodegradable at the end of their lifecycle have recently become promising materials (Arrieta, 2021; Immergut and Mark, 1965; D. Li et al., 2018; Ljungberg and Wesslén, 2005; Sears, 1982; A. Wypych, 2017; G. Wypych, 2017).

Perlite (Pe) is a glassy, aluminosilicate dominant volcanic mineral that can expand when exposed to heat due to its water retaining capacity. It is available in both virgin and expanded forms. Expanded perlite is used for various purposes, ranging from construction to horticulture, due to its chemical composition, inertness to many chemicals, low density, and thermal stability. The water content changes from 2 to 5 wt.% (Aksoy et al., 2022; Doğan and Alkan, 2004; Kabra et al., 2013; Maxim et al., 2014). Perlite can also be used as a filler for polymer composites.

When examining Pe/PLA composites, we find that there are very few studies available. In one of these studies, Pe/PLA composites were prepared through in-situ polymerization (Eğri, 2019). In the study direct condensation polymerization of PLA was carried out using perlite and lactic acid. The amount of perlite used ranged from 0.4% to 1.2% by weight, with the aim of enhancing the thermal stability of PLA. Morphological, thermal and structural properties were analyzed. Addition of Pe into the polymerization medium resulted in higher molecular weight and degree of crystallinity. Additionally, perlite led to an increase in thermal stability, which was assumed to result from a higher molecular weight and a higher degree of crystallinity due to improved chain orientation (Eğri, 2019). In another study, Pe/PLA composites were prepared by solution casting and melt processing, and their performance was compared with montmorillonite filled PLA composites. Type and concentration of the filler were found to be significant in some cases such as T_g, morphology and mechanical properties. It was also reported that mixing was found to affect morphological and thermal properties. Dynamic mechanical properties such as loss and storage modulus were reported to increase by the addition of perlite and montmorillonite. Although detailed characterization was performed thermal degradation behavior of the composites were not investigated (Tian and Tagaya, 2007). As can be seen from the existing literature, the properties of perlite-containing composites prepared with plasticized PLA (pPLA) and unplasticized PLA have not been investigated before. In this study, Pe/PLA, Pe/pPLA composites were prepared, and their morphological, structural, thermal, and mechanical properties were investigated. PLA polymer used in the study is derived from corn, a sustainable agricultural product. Perlite (Pe) is a mineral extracted from the ground, while glycerol, which can be produced through biological processes, is biodegradable and available in food-grade purity.

Materials and Methods

PLA (Luminy LX175) and perlite were kindly supplied by Total Corbion and Genper Expanded Perlite Industry Business Co. respectively. Chloroform and glycerol were purchased from Merck-Millipore. All chemicals were used as received without any purification. The particle size distribution histogram and light microscope images of perlite can be seen from Fig. 1. The average particle size of perlite was 33.6 µm.

Table 1. Sample codes and contents.

Sample Codes	PLA (wt.%)	Glycerol (wt.%)	Perlite (wt.%)
PLA	100	-	-
pPLA	90	10	-
5Pe/95PLA	95	-	5
10Pe/90PLA	90	-	10
15Pe/85PLA	85	-	15
20Pe/80PLA	80	-	20
5Pe/95pPLA	85.5	9.5	5
10Pe/90pPLA	81	9	10
15Pe/85pPLA	76.5	8.5	15
20Pe/80pPLA	72	8	20

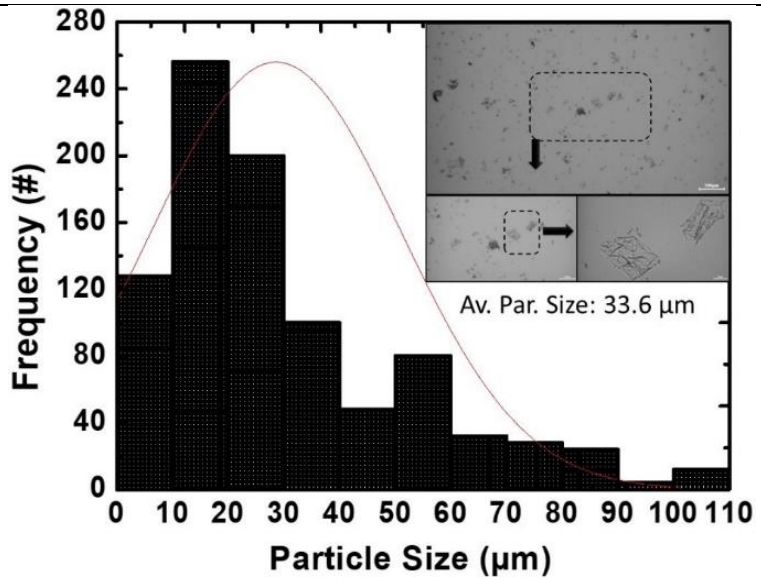

Fig. 1. Particle size distribution histogram of perlite (inset: optical microscope images of perlite at different magnifications. Scale bars are 100, 50 and 10 µm, respectively)

Preparation of Pe/PLA and Pe/pPLA composites:
PLA and perlite were dried in a vacuum oven (Wisd, WOV-20) at 80°C for 12 h to remove the residual moisture. Chloroform was the solvent and 10 wt.% of PLA containing stock solution was prepared at room temperature by a magnetic stirrer (Daihan MSH 20 D, 450 rpm) overnight. Two sets of samples were prepared: PLA-based samples and pPLA-based samples. In both groups, the ratio of perlite was 0%, 5%, 10%, 15%, and 20% by weight. Sample codes and contents of the samples are listed in Table 1.

The preparation steps of the composites are illustrated in Fig.2. PLA composites were prepared by one-step mixing process, combining the PLA/chloroform solution and perlite using a high shear mixer (KuraboMazerustar KK250, 1600 rpm) for 90 seconds. The samples were cast into the Petri dishes and dried at room temperature for one day in a closed chamber under vacuum. The next day, samples were further dried in an oven (Wisd, WOV-20) at 45°C for 15 h. To achieve a homogeneous film morphology, the cast films were compression molded between Teflon-coated plates at 200°C for 60 sec under 3 MPa pressure and cooled to 25°C for 2 minutes. For the pPLA composites, glycerol was added into the PLA solution and mixed for 30 min. using a magnetic stirrer (Daihan MSH 20 D, 450 rpm). The ratio of was 10 wt.% glycerol in PLA-glycerol mixture. The subsequent steps were performed in the same manner as for the PLA composites.

Morphological Analysis:
An optical microscope (AmScope 40X-2500X LED) was used to determine the average particle size of perlite. The composite morphology was analyzed using a field emission scanning electron microscopy (FESEM) at 30 kV (JEOL JSM-6400). Composites were cryofractured in liquid nitrogen and then sputter-coated with a 3-6 nm layer of Au/Pd alloy for cross-sectional investigation.

Fourier Transform Infrared Spectroscopy (FTIR):
Attenuated total internal reflectance (ATR mode) spectroscopy was performed for structural analysis of the samples (Perkin Elmer, Spectrum 100 IR spectrometer). Spectra were recorded in the transmittance mode between 400 and 4000 cm^{-1}, spectral resolution of 4 cm^{-1} at a scan rate of 4 scans.

Thermogravimetric Analysis (TGA):
In order to determine thermal degradation behavior of the samples, TGA analysis was carried out (Seiko, TG/DTA 6300) between 25 and 600°C. Temperature rate was 10°C min^{-1} under 200 ml min^{-1} N_2 flow rate.

Differential Scanning Calorimetry (DSC):
DSC analysis was performed under N_2 atmosphere with heating/cooling rate of 10°C min^{-1} from -70 to 200°C (Perkin Elmer Diamond).

Mechanical Characterization:
Mechanical properties of PLA and pPLA-based samples were determined using a universal mechanical testing system (Devotrans, DVT GPU/RD) with the test speed of 50 mm min^{-1}. Samples were cut by a blade (width x length →5 mm x 15 mm). Before the test, thickness of the samples was measured using digital thickness meter (Asimeto).

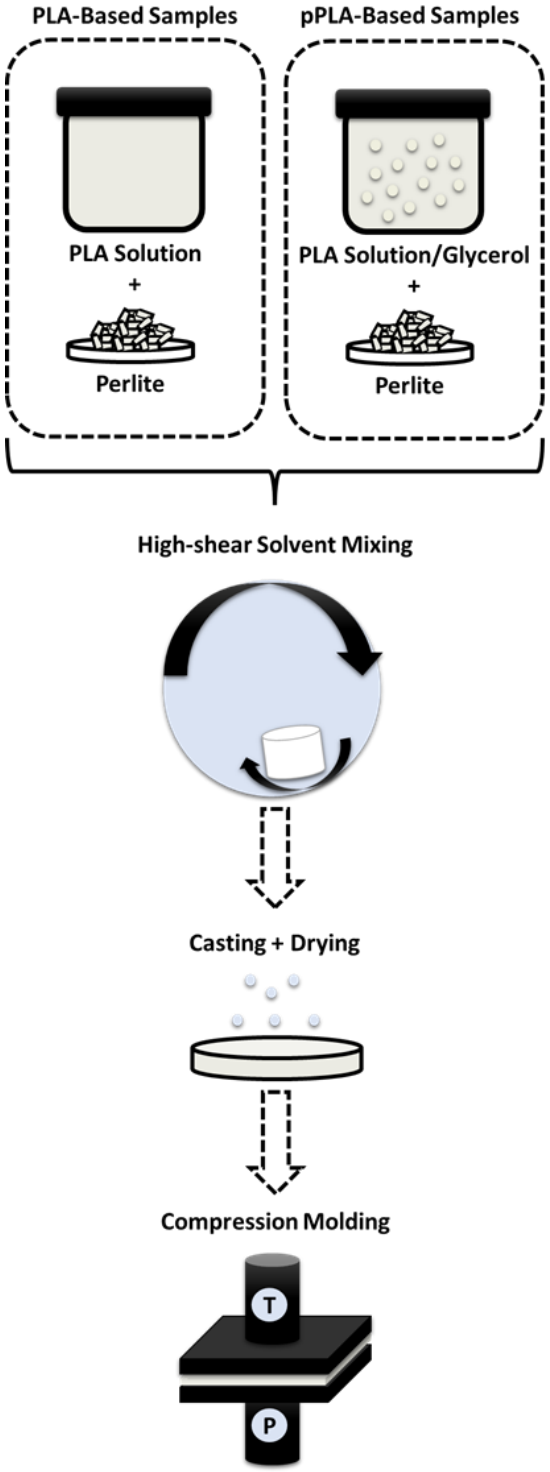

Fig. 2. Sample preparation route.

Results
Morphological Analysis

FESEM images of PLA, 5Pe/PLA, 20Pe/80PLA, pPLA, 5Pe/95pPLA, 20Pe/80pPLA, can be seen from Fig. 3a to 3f, respectively. Samples were analyzed by considering the cross-sectional micromorphology in terms of melting,

plasticization, filler-matrix interaction, geometry, distribution, and orientation of the filler. As mentioned in the method, films were prepared at 200°C. That was determined based on the film formation of 20Pe/80PLA, the sample with the highest Pe content without any plasticizer. As known, plasticizers lower the T_g and T_m, which results in reduced processing temperatures. Although PLA, 5Pe/95PLA, pPLA and 5Pe/95pPLA, 20Pe/80pPLA could be processed around 190-195°C, higher temperature was required for 20Pe/80PLA due to its higher inorganic solid Pe content. Fig. 3a shows the virgin PLA, where complete melting is evident at 200°C. Fig. 3b and 3c display the 5Pe95/PLA and 20Pe/80PLA composites, respectively. In both images, Pe particles can be seen clearly. At higher filler concentration, agglomerations of Pe particles are visible in Fig. 3c. In Fig. 3d, the pPLA shows numerous voids, likely resulting from phase separation and the vaporization of glycerol (Almazrouei et al., 2017, 2022; Dou et al., 2009; Halloran et al., 2022), as explained in the TGA analysis section. In Fig. 3e (5Pe/95pPLA), Pe particles showed random orientation throughout the cross-section of the composite with good dispersion. In Fig. 3f (20Pe/80pPLA), the agglomerations of Pe can be due to higher Pe content. The number of voids can be given as pPLA >5Pe/95pPLA>20Pe/80pPLA. This behavior was likely caused by the composition and thermal stability of the composites. Since pPLA had the highest amount of glycerol, it experienced greater phase separation and vaporization. On the other hand, for Pe-filled pPLA, glycerol amount is lower than pPLA, resulting in reduced phase separation and vaporization.

Fourier Transform Infrared Spectroscopy (FTIR)

Fig. 4 shows FTIR spectra of all samples. From Fig. 4b, the plastization effect on PLA by glycerol can be seen in detail. The peaks observed at 955, 866, and 754 cm^{-1} correspond to stretching vibrations of C-C and C–H bonds. The peaks observed at 1128, 1081, and 1043 cm^{-1} are attributed to the deformation vibrations of C-O bonds in CH-O groups within PLA. The peaks detected at 1268 and 1181 cm^{-1} are a result of stretching vibrations in C–C bonds and symmetric stretching vibrations in C–O–C bonds within ester groups present in PLA. The peaks observed at 1383, 1365, and 1360 cm^{-1} correspond to -CH- deformation, stretching vibrations of methyl groups' C-H bonds, and bending vibrations of $-CH_3$ bonds. The vibration of $-CH_3$ bonds' deformation is detected at 1455 cm^{-1}, while stretching vibrations of -C-H bonds are identified at 2996 and 2946 cm^{-1}.

Additionally, the peak at 1748 cm^{-1} is attributed to stretching vibrations of the carbonyl group's -C=O bonds (Ekiz et al., 2022; Muller et al., 2017; Pop et al., 2019). The spectrum of pPLA is primarily characterized by a broad band at 3300 cm^{-1}, indicating the stretching vibration modes of -OH groups associated with glycerol and adsorbed water (Cetin et al., 2022). The presence of interactions between PLA and the plasticizer can be detected through shifts in specific bands: from 1748 to 1749 cm^{-1}, 1181 to 1182 cm^{-1}, 1128 to 1126 cm^{-1}, 1081 to 1082 cm^{-1}, and 2946 to 2944 cm^{-1}. These changes in the absorption bands may show how PLA and the plasticizers interact and are miscible (Chieng, Ibrahim, Then, et al., 2014).

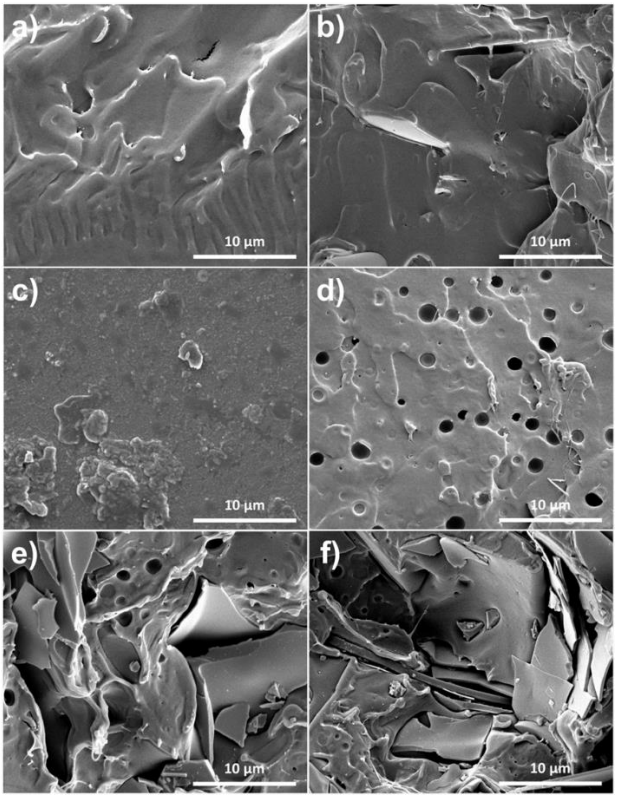

Fig. 3. FESEM images of a) PLA, b) 5Pe/95PLA, c) 20Pe/80PLA, d) pPLA, e) 5Pe/95pPLA, f) 20Pe/80pPLA

Fig. 4c shows FTIR spectra of perlite powder in the range of 450 – 2000 cm^{-1}. Three major peaks around 783, 1020, and 1624 cm^{-1} are associated with characteristic peaks of perlite. The peak at 1624 cm^{-1} is assigned to bending vibration (δ) of absorbed molecular water in perlite. Asymmetric stretching vibrations (v_{as}) of Si-O-Si is observed at 1020 cm^{-1}. Symmetric stretching vibrations (v_s) of Si-O-M (M: Al or Si) is also observed at 783 cm^{-1}. At lower wavenumbers (such as 732 and 567 cm^{-1}), characteristic peaks of glass, quartz and feldspar are observed. The distinct peak at 443 cm^{-1} is attributed to silicates in perlite (Aksoy et al., 2022; Eğri, 2019; Jing et al., 2011; Kaufhold et al., 2014; Sodeyama et al., 1999; Szostak and Thomas, 1986). As seen from Fig. 4d, the peaks observed in both pPLA and 20Pe/80pPLA composites are nearly identical to those of pure PLA. This suggests that there are no new bonds formed or significant chemical interactions occurring within the blend or composites (Chieng, Ibrahim, Yunus, et al., 2014).

Thermogravimetric Analysis (TGA)

Thermal degradation behavior of the perlite, PLA, 5Pe/95PLA, 20Pe/80PLA, 5Pe/95pPLA, 20Pe/80pPLA between 25 and 600°C can be seen in Fig. 5 a-c. PLA showed a wide characteristic plateau and one-step thermal degradation started after 300°C and it showed an accelerating, degradation after 340°C with a T_{max} value around 366°C as previously reported (Ekiz et al., 2022).

The residual ash content of PLA was 0.35 wt.%. On the other hand, pPLA showed two-step thermal degradation caused by degradation behavior of glycerol (Almazrouei

et al., 2017; Dou et al., 2009; Maizatul et al., 2013). As previously reported by Dou et al., most of the weight loss was observed in the range between 150 and 280°C and the ratio was around 95 wt.%.

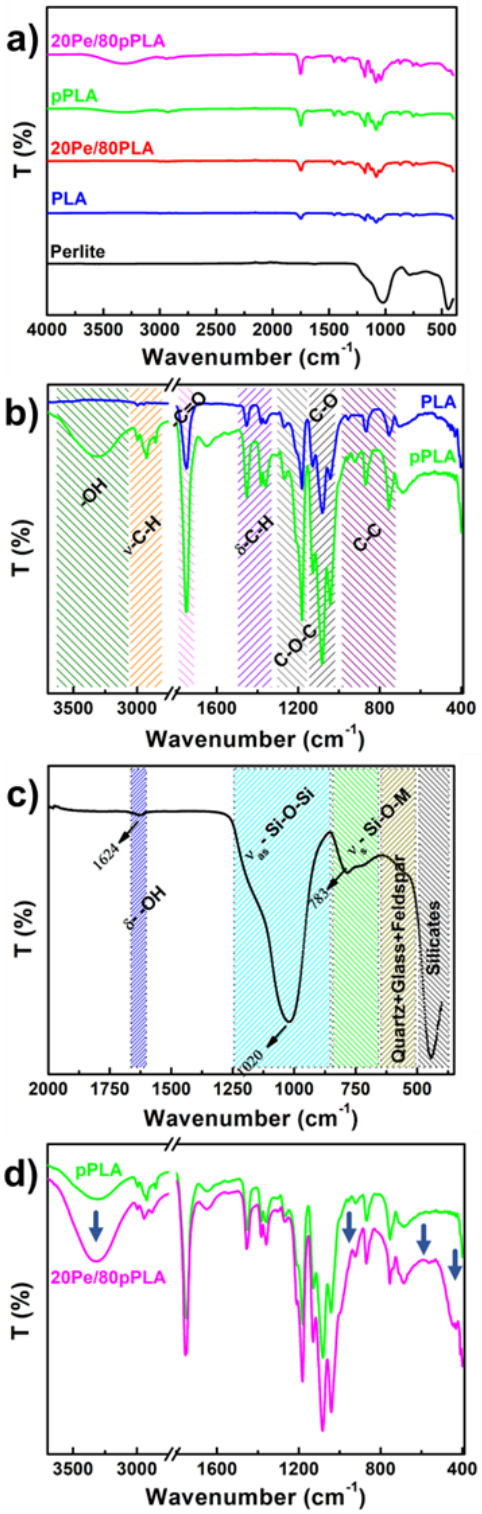

Fig. 4. FTIR spectra of a) all samples, b) PLA and pPLA films, c) perlite powder, and d) pPLA and 20Pe/80pPLA composite films.

The residual ash content was determined around 2 wt.% in the case of further heating (Almazrouei et al., 2017; Dou et al., 2009). As given in Table 1 glycerol content of pPLA was 10 wt.% and the weight loss was 5 and 10 wt.% at 150 and 270°C respectively that was parallel with the previous findings. The residual ash content was approximately 2.5 wt.% for pPLA, where the PLA/glycerol ratio was 0.35/2.15. This result is also in good agreement with the literature (Dou et al., 2009). As obvious from Fig 5b and c, perlite did not show thermal degradation between 25 and 600°C due to its chemical composition in which SiO_2 is the dominant phase. It showed a wide plateau with the T_{max} value around 216°C with the weight loss around 3 wt.% at this temperature and the total weight loss of 6wt.% at 600°C. As reported in the literature, while the weight loss at the initial temperature range between 20–250°C was associated with the removal of moisture trapped on the perlite surface; the reduction in weight between 250-500°C was indication of chemically bound water (Aksoy et al., 2022). PLA and Pe/PLA composites showed almost similar thermal degradation behavior.

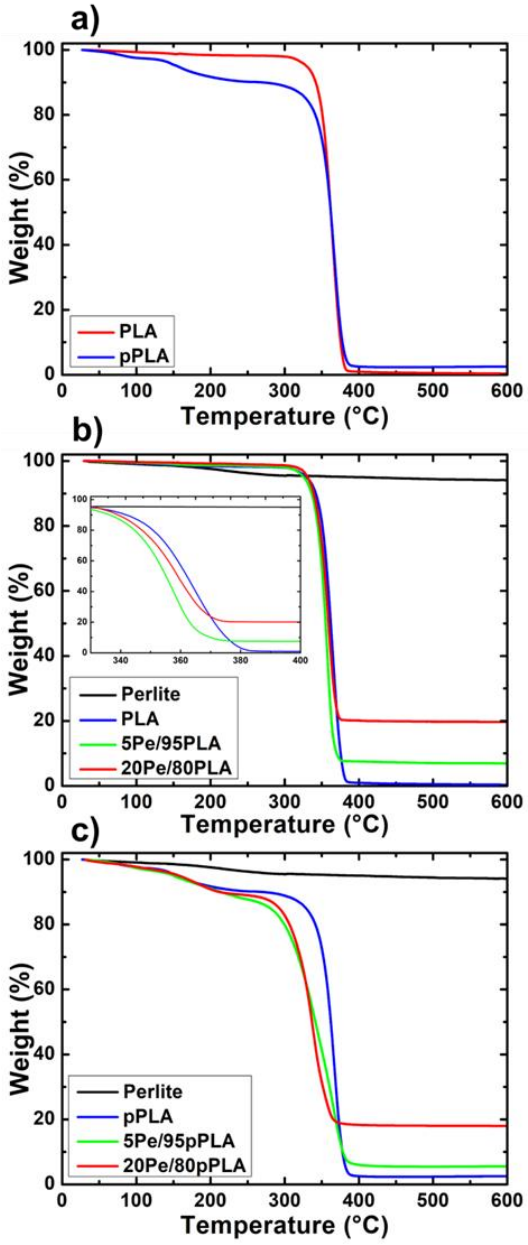

Fig. 5. TGA graphs of a) PLA and pPLA, b) Pe and Pe/PLA composites, c) Pe and Pe/pPLA composites.

However, as shown in the inset of Fig. 5b, the composites exhibited relatively higher weight loss compared to PLA. This was likely due to the removal of water from the

perlite as explained previously. The ash contents of PLA, 5Pe/95PLA and 20Pe/80PLA were determined as respectively 0.35, 6.9, 19.7 wt.% at 600°C. Although pPLA and Pe/pPLA composites showed two-step degradation profile, the composites showed relatively higher weight loss compared to pPLA. This was likely due to the synergistic interaction of glycerol and water present in perlite.

As given in Table 1, the glycerol contents of pPLA, 5Pe/95pPLA and 20Pe/80pPLA were as 10, 9.5, and 8 wt.%, respectively. The weight loss at 270°C for perlite, pPLA, 5Pe/95pPLA and 20Pe/80pPLA as 4.2, 10, 13.7 and 11.8 wt.%, respectively. As can be seen, Pe/PLA composites showed higher weight loss due to the degradation of glycerol and the removal of water in perlite. Since 20Pe/80pPLA had a lower glycerol content compared to 5Pe/95pPLA, the weight loss was slightly higher for 5Pe/95pPLA. The ash contents of pPLA, 5Pe/95pPLA and 20Pe/80pPLA at 600°C were determined as respectively 2.5, 5.6, and 18 wt.%, respectively. To increase the thermal stability of the Pe/PLA composites, the water content must be considered, and calculations should be performed accordingly.

Differential Scanning Calorimetry (DSC)

The thermal behavior of PLA, pPLA, 20Pe/80PLA, and 20Pe/80pPLA films as a function of temperature is presented in Fig. 6. The thermal parameters, including glass transition temperature (T_g), cold crystallization temperature (T_{cc}), cold crystallization enthalpy (ΔH_{cc}), melting temperature (T_m), melting enthalpy (ΔH_m) values of the samples, and crystallinity of PLA (X_{PLA}) were determined from the extracted data in Fig. 6 and given in Table 2. Since the 1st heating and cooling was carried out for creating similar thermal history to all samples, the discussion was given based on 2nd heating of all samples. T_{cc} and T_m were obtained from the peak value of cold crystallization exotherm and melting endotherm, respectively. The degree of crystallinity values for neat PLA and pPLA composites were calculated from the following formula:

$$X_{PLA}(\%) = \frac{(\Delta H_m - \Delta H_{cc})}{(\Delta H_m^o * w)} * 100$$

where ΔH_m^0 and w are melting enthalpy of 100% crystalline PLA, and weight fraction of PLA in the composite, respectively. According to literature, ΔH_m^0 of PLA was assumed to be 93 J g^{-1} (Ferri et al., 2017).

PLA is a semi-crystalline polymer and T_g, cold crystallization exotherm, melting endotherm peaks were observed and neat PLA exhibited a glass transition temperature (T_g) of 57.11°C. The cold crystallization occurred between 100 and 125°C and the T_{cc} was measured as 112.78°C from the maximum value of cold crystallization exotherm peak. The melting occurred between 135 and 155°C and a single T_m was measured as 148.16°C from the peak of melting endotherm which is parallel with the previous studies (Velghe et al., 2023; Zhai et al., 2009). X_{PLA} value for PLA was calculated as 4.34%. In the case of pPLA films, T_g, and T_{cc} were decreased to 53.93 and 105.4°C with the incorporation of plasticizer. The cold crystallization occurred between 90 and 120°C. As previously described by Li and Huneault, cold crystallization occurred with lower energy content as a result of increased chain mobility brought on by the plasticization effect, which results in lower cold crystallization temperatures (H. Li and Huneault, 2007). As seen from Fig. 6a, two distinct melting peaks were observed as 141.37 and 148.72°C, respectively. This phenomenon might be related to two different kinds of PLA crystals with different lamellae thicknesses (Di Lorenzo and Androsch, 2019; Fortunati et al., 2012; Su et al., 2009).

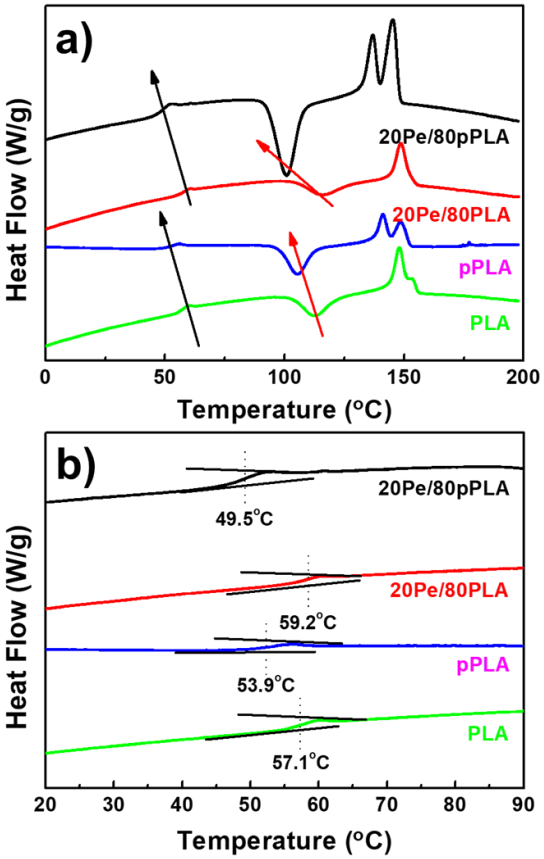

Fig. 6. a) DSC thermograms of PLA, p-PLA, 20per-PLA, and 20per-p-PLA films between 0 and 200°C. b) Detailed view of glass transition temperature in the range of 20 - 90°C.

For 20Pe/80PLA composite, T_g, and T_{cc} values were increased to 59.19 and 116.59°C, respectively. Also, a distinct melting peak was observed at 148.79°C. As seen from Table 2 and Fig. 6, 20Pe/80PLA composite exhibited a more pronounced increase in crystallinity due to incorporation of perlite into composite. Perlite could effectively serve as cold crystallization nucleation sites (Chen et al., 2015; Papageorgiou et al., 2014; Tarani et al., 2021).

Interestingly, T_g, T_{cc} T_{m1}, and T_{m2} values of 20Pe/80pPLA composite decreased to 49.53, 100.97, 136.98, and 145.41°C, which are lower than neat PLA. In parallel with the literature, crystallinity of 20Pe/80pPLA composite increased from 5.57% to 9.93%, and it was also observed

that the second melting peak became more pronounced with the addition of plasticizer (Gumus et al., 2012a). This might be related to the synergistic effect of the filler and plasticizer to increase the segmental movement of PLA macromolecules by providing higher chain mobility and free volume (Chen et al., 2015; Gumus et al., 2012b).

Table 2. Thermal parameters of PLA, p-PLA, 20per-PLA and 20per-p-PLAfilms from DSC data @2nd run

Sample Code	T_g (ºC)	T_{cc} (ºC)	ΔH_{cc} (J/g)	T_m (ºC)	ΔH_m (J/g)	X_{PLA} (%)
PLA	57.11	112.78	27.33	148.16	31.37	4.34
pPLA	53.93	105.40	34.76	141.37 148.72	31.86	3.12
20Pe/80PLA	59.19	116.59	20.21	148.79	24.36	5.57
20Pe/80pPLA	49.53	100.97	24.88	136.98 145.41	31.54	9.93

Table 3. Mechanical properties of samples

Sample Code	Tensile Strength (MPa)	Tensile Strain (%)
PLA	41.72	7.09
pPLA	37.51	8.01
5Pe/95PLA	30.00	4.72
10Pe/90PLA	30.27	5.27
15Pe/85PLA	31.22	5.11
20Pe/80PLA	34.56	6.91
5Pe/95pPLA	23.81	7.87
10Pe/90pPLA	20.47	7.69
15Pe/85pPLA	22.61	10.74
20Pe/80pPLA	N.A.	N.A.

Mechanical Characterization

Mechanical analysis results of the samples can be seen in Table 3. The tensile strength/tensile strain of PLA and pPLA were measured as 41.72/7.09, 37.51/8.01 MPa/%, respectively. As can be seen from these outcomes, tensile strength decreased and elongation at break increased with the addition of plasticizer. Glycerol behaved like the plasticizer by increasing the free volume and chain mobility. As a result of these, flexibility of the pPLA and elongation at break increased (Halloran et al., 2022; Immergut and Mark, 1965; Jacobsen and Fritz, 1999; Maiza, 2015; Mousa et al., 2022; Sears, 1982; A. Wypych, 2017; G. Wypych, 2017).

The tensile strength/tensile strain of PLA, 5Pe/95PLA, 10Pe/90PLA and 15Pe/85PLA samples were measured as 41.72/7.09, 30/4.72, 30.27/5.27 and 31.22/5.11 MPa/%, respectively. The tensile strength and elongation at break for composites decreased compared to PLA. A decrease of 25-30% in tensile strength was observed with the addition of perlite. That was assumed to be due to insufficient interaction between matrix and filler. As shown in FESEM images, perlite agglomerations formed at higher concentrations, and these agglomerates created weak points in the composite. These agglomerates disrupted the continuity of the polymer matrix in the composite, leading to a decrease in tensile strength. The tensile strength/tensile strain of pPLA, 5Pe/95pPLA, 10Pe/90pPLA and 15Pe/85pPLA were 37.51/8.01, 23.81/7.87, 20.47/7.69 and 22.61/10.74 MPa/%, respectively. The tensile strength of the specimens decreased while the elongation at break values increased compared to the unplasticized samples. For the 20 wt.% Pe filled samples, repeatable measurements could not be performed due to high level of perlite agglomeration.

Discussion and Conclusion

The aim of this study was to prepare composites consisting of sustainable, biodegradable materials that serve as environmentally friendly alternatives. In this context, two different sets of samples were prepared. The first group consisted of perlite-filled PLA composites, which were made using a combination of solution casting and compression molding techniques. In the second set, PLA was plasticized with glycerol, and perlite-filled pPLA composites were prepared using the same method as for the PLA composites. Morphological, chemical, thermal, and mechanical characterizations were performed. The morphological analysis showed that homogeneous PLA and pPLA films were obtained. However, phase separation and volatilization of glycerol were observed in the pPLA-based samples. Pe was found to exhibit homogeneous dispersion at low filler concentrations, while agglomerations were observed at higher Pe concentrations. FTIR analysis indicated that the chemical structure of PLA was altered by plasticization with glycerol, and the incorporation of perlite led to the formation of characteristic perlite peaks in the composite spectra. TGA analysis revealed that plasticization of PLA resulted in lower thermal stability due to a reduction in molecular weight. Additionally, perlite did not significantly contribute to the thermal stability in either group, likely due to its water content.

When the mechanical properties were examined, the tensile strength of PLA decreased after plasticization, on

the other hand elongation at break and flexibility increased because of increased mobility within the macromolecular chains. Similarly, the tensile strength of Pe/pPLA composites showed lower mechanical strength compared to Pe/PLA composites due to plasticizing effect of glycerol. Since developing materials within the scope of sustainable engineering is becoming increasingly important, future work will focus on extending the study with different types of plasticizers.

Acknowledgements

This project was funded by Yalova University, BAP (Scientific Research Project) Project No and Title: 2023/YL/0007, Preparation and Characterization of Perlite Filled Poly(lactide acid) Composites.

References

Aksoy, Ö., Alyamaç, E., Mocan, M., Sütçü, M., Özveren-Uçar, N., Seydibeyoğlu, M. Ö. (2022). Characterization of perlite powders from Izmir, Türkiye region. *Physicochemical Problems of Mineral Processing*, *58(6)*, 155277.

Almazrouei, M., Adeyemi, I., Janajreh, I. (2022). Thermogravimetric assessment of the thermal degradation during combustion of crude and pure glycerol. *Biomass Conversion and Biorefinery*, *12(10)*, 4403-4417.

Almazrouei, M., Samad, T. El, Janajreh, I. (2017). Thermogravimetric Kinetics and High Fidelity Analysis of Crude Glycerol. *Energy Procedia*, *142*, 1699-1705.

Al-Mulla, E. A. J., Yunus, W. M. Z. W., Ibrahim, N. A. B., Rahman, M. Z. A. (2010). Properties of epoxidized palm oil plasticized polytlactic acid. *Journal of Materials Science*, *45(7)*, 1942-1946.

Arrieta, M. P. (2021). Influence of plasticizers on the compostability of polylactic acid. *Journal of Applied Research in Technology Engineering*, *2(1)*, 1-9.

Carpintero, M., Marcet, I., Rendueles, M., Díaz, M. (2022). Egg Yolk Oil as a Plasticizer for Polylactic Acid Films. *Membranes*, *12(1)*, 46.

Cetin, M. S., Aydogdu, R. B., Toprakci, O., Karahan Toprakci, H. A. (2022). Sustainable, Tree-Free, PLA Coated, Biodegradable, Barrier Papers from Kendir (Turkish Hemp). *Journal of Natural Fibers*, *19*(16), 13802–13814.

Chen, P., Zhou, H., Liu, W., Zhang, M., Du, Z., Wang, X. (2015). The synergistic effect of zinc oxide and phenylphosphonic acid zinc salt on the crystallization behavior of poly (lactic acid). *Polymer Degradation and Stability*, *122*, 25-35.

Chieng, B. W., Ibrahim, N. A., Then, Y. Y., Loo, Y. Y. (2014). Epoxidized vegetable oils plasticized poly(lactic acid) biocomposites: Mechanical, thermal and morphology properties. *Molecules*, *19(10)*, 16024-16038.

Chieng, B. W., Ibrahim, N. A., Yunus, W. M. Z. W., Hussein, M. Z. (2014). Poly(lactic acid)/poly(ethylene glycol) polymer nanocomposites: Effects of graphene nanoplatelets. *Polymers*, *6(1)*, 93-104.

Di Lorenzo, M. L., Androsch, R. (2019). Influence of α′-/α-crystal polymorphism on properties of poly(l-lactic acid). *Polymer International*, *68(3)*, 320-334.

Doğan, M., Alkan, M. (2004). Some physicochemical properties of perlite as an adsorbent. *Fresenius Environmental Bulletin*, *13(3B)*, 251-257.

Dou, B., Dupont, V., Williams, P. T., Chen, H., Ding, Y. (2009). Thermogravimetric kinetics of crude glycerol. *Bioresource Technology*, *100(9)*, 2613-2620.

Eğri, Ö. (2019). Use of microperlite in direct polymerization of lactic acid. *International Journal of Polymer Analysis and Characterization*, *24(2)*, 142-149.

Ekiz, I., Cetin, M. S., Toprakci, O., Toprakci, H. A. K. (2022). Effects of S/EB ratio on some properties of PLA/SEBS blends. *Bulletin of Materials Science*, *45(4)*, 251.

Ferri, J. M., Garcia-Garcia, D., Montanes, N., Fenollar, O., Balart, R. (2017). The effect of maleinized linseed oil as biobased plasticizer in poly(lactic acid)-based formulations. *Polymer International*, *66*(6), 882–891.

Fortunati, E., Armentano, I., Zhou, Q., Puglia, D., Terenzi, A., Berglund, L. A., Kenny, J. M. (2012). Microstructure and nonisothermal cold crystallization of PLA composites based on silver nanoparticles and nanocrystalline cellulose. *Polymer Degradation and Stability*, *97(10)*, 2027-2036.

Grigale, Z., Kalnins, M., Dzene, A., Tupureina, V. (2010). Biodegradable Plasticized Poly(lactic acid) Films. *Scientific Journal of Riga Technical University Material Science and Applied Chemistry*, *21*, 97–103.

Gumus, S., Ozkoc, G., Aytac, A. (2012a). Plasticized and unplasticized PLA/organoclay nanocomposites: Short- and long-term thermal properties, morphology, and nonisothermal crystallization behavior. *Journal of Applied Polymer Science*, *123*(5), 2837–2848.

Gumus, S., Ozkoc, G., Aytac, A. (2012b). Plasticized and unplasticized PLA/organoclay nanocomposites: Short- and long-term thermal properties, morphology, and nonisothermal crystallization behavior. *Journal of Applied Polymer Science*, *123(5)*, 2837-2848.

Halász, K., Csóka, L. (2013). Plasticized Biodegradable Poly(lactic acid) Based Composites Containing Cellulose in Micro- and Nanosize. *Journal of Engineering (United Kingdom)*, *2013*, 329379.

Halloran, M. W., Danielczak, L., Nicell, J. A., Leask, R. L., Marić, M. (2022). Highly Flexible Polylactide Food Packaging Plasticized with Nontoxic, Biosourced Glycerol Plasticizers. *ACS Applied Polymer Materials*, *4(5)*, 3608-3617.

Immergut, E. H., Mark, H. F. (1965). Principles of Plasticization. *Advances in Chemistry*, *48*, 1-29

Jacobsen, S., Fritz, H. G. (1999). Plasticizing polylactide - the effect of different plasticizers on the mechanical properties. *Polymer Engineering and Science*, *39*(7), 1303.

Jing, Q., Fang, L., Liu, H., Liu, P. (2011). Preparation of surface-vitrified micron sphere using perlite from Xinyang, China. *Applied Clay Science*, *53(4)*, 745-748.

Kabra, S., Katara, S., Rani, A. (2013). Characterization and Study of Turkish Perlite. *International Journal of*

Innovative Research in Science, Engineering and Technology, *2(9)*, 4319-4326.

Kantee, J., Kajorncheappunngam, S. (2017). Properties of plasticized polylactic acid films with epoxidized rubber seed oil. *Chiang Mai Journal of Science*, *44(4)*, 1591-1600.

Kaufhold, S., Reese, A., Schwiebacher, W., Dohrmann, R., Grathoff, G. H., Warr, L. N., Halisch, M., Müller, C., Schwarz-Schampera, U., Ufer, K. (2014). Porosity and distribution of water in perlite from the island of Milos, Greece. *Journal of the Korean Physical Society*, *3(1)*, 598.

Li, D., Jiang, Y., Lv, S., Liu, X., Gu, J., Chen, Q., Zhang, Y. (2018). Preparation of plasticized poly (lactic acid) and its influence on the properties of composite materials. *PLoS ONE*, *13(3)*, 1-15.

Li, H., Huneault, M. A. (2007). Effect of nucleation and plasticization on the crystallization of poly(lactic acid). *Polymer*, *48(23)*, 6855-6866.

Ljungberg, N., Wesslén, B. (2005). Preparation and properties of plasticized poly(lactic acid) films. *Biomacromolecules*, *6(3)*, 1789-1796.

Maiza, M. 'Benaniba, M. T. 'Quintard, G. 'Massardier-N. V. (2015). Biobased additive plasticizing Polylactic acid (PLA). . *Polimeros* , *25*, 581–590.

Maizatul, N., Norazowa, I., Yunus, W. M. Z. W., Khalina, A., Khalisanni, K. (2013). FTIR and TGA analysis of biodegradable poly(lactic acid)/treated kenaf bast fibre: Effect of plasticizers. *Pertanika Journal of Science and Technology*, *21(1)*, 151-160.

Martino, V. P., Jiménez, A., Ruseckaite, R. A. (2009). Processing and characterization of poly(lactic acid) films plasticized with commercial adipates. *Journal of Applied Polymer Science*, *112(4)*, 2010-2018.

Maxim, L. D., Niebo, R., Mcconnell, E. E. (2014). Perlite toxicology and epidemiology - A review. *Inhalation Toxicology*, *26(5)*, 259-270.

Mousa, N., Galiwango, E., Haris, S., Al-marzouqi, A. H., Abu-jdayil, B., Caires, Y. L. (2022). A New Green Composite Based on Plasticized Polylactic Acid Mixed with Date Palm Waste for Single-Use Plastics Applications. *Polymers*, *14(3)*, 574.

Muller, J., González-Martínez, C., Chiralt, A. (2017). Poly(lactic) acid (PLA) and starch bilayer films, containing cinnamaldehyde, obtained by compression moulding. *European Polymer Journal*, *95*, 56–70.

Papageorgiou, G. Z., Terzopoulou, Z., Bikiaris, D., Triantafyllidis, K. S., Diamanti, E., Gournis, D., Klonos, P., Giannoulidis, E., Pissis, P. (2014). Evaluation of the formed interface in biodegradable poly(l-lactic acid)/graphene oxide nanocomposites and the effect of nanofillers on mechanical and thermal properties. *Thermochimica Acta*, *597*, 48-57.

Pop, M. A., Croitoru, C., Bedő, T., Geaman, V., Radomir, I., Coșnița, M., Zaharia, S. M., Chicoș, L. A., Miloșan, I. (2019). Structural changes during 3D printing of bioderived and synthetic thermoplastic materials. *Journal of Applied Polymer Science*, *136(17)*, 47382.

Sears, J. K. and D. J. R. (1982). The Technology of plasticizers. *Journal of Polymer Science: Polymer Letters Edition*, *20(8)*, 459.

Sodeyama, K., Sakka, Y., Kamino, Y., Seki, H. (1999). Preparation of fine expanded perlite. *Journal of Materials Science*, *34(10)*, 2461-2468.

Su, Z., Liu, Y., Guo, W., Li, Q., Wu, C. (2009). Crystallization behavior of poly(lactic acid) filled with modified carbon black. *Journal of Macromolecular Science, Part B: Physics*, *48(4)*, 670-683.

Szostak, R., Thomas, T. L. (1986). Reassessment of zeolite and molecular sieve framework infrared vibrations. *Journal of Catalysis*, *101(2)*, 549-552.

Tarani, E., Pušnik Črešnar, K., Zemljič, L. F., Chrissafis, K., Papageorgiou, G. Z., Lambropoulou, D., Zamboulis, A., Bikiaris, D. N., Terzopoulou, Z. (2021). Cold crystallization kinetics and thermal degradation of pla composites with metal oxide nanofillers. *Applied Sciences (Switzerland)*, *11(7)*, 3004.

Tian, H., Tagaya, H. (2007). Preparation, characterization and mechanical properties of the polylactide/perlite and the polylactide/montmorillonite composites. *Journal of Materials Science*, *42(9)*, 3244-3250.

Velghe, I., Buffel, B., Vandeginste, V., Thielemans, W., Desplentere, F. (2023). Review on the Degradation of Poly(lactic acid) during Melt Processing. *Polymers*, *15(9)*, 2047.

Wypych, A. (2017). *Databook of Plasticizers*. Toronto: ChemTec Publishing.

Wypych, G. (2017). *Handbook of plasticisers*. Toronto: ChemTec Publishing.

Xu, Y. Q., Qu, J. P. (2009). Mechanical and rheological properties of epoxidized soybean oil plasticized poly(lactic acid). *Journal of Applied Polymer Science*, *112(6)*, 3185-3191.

YousefniaPasha, H., Mohtasebi, S. S., Tabatabaeekoloor, R., Taherimehr, M., Javadi, A., Soltani Firouz, M. (2021). Preparation and characterization of the plasticized polylactic acid films produced by the solvent-casting method for food packaging applications. *Journal of Food Processing and Preservation*, *45(12)*, e16089.

Yuan, Y., Hu, Z., Fu, X., Jiang, L., Xiao, Y., Hu, K., Yan, P., Lei, J. (2016). Poly(lactic acid) plasticized by biodegradable glyceryl lactate. *Journal of Applied Polymer Science*, *133(21)*, 43460.

Zhai, W., Ko, Y., Zhu, W., Wong, A., Park, C. B. (2009). A study of the crystallization, melting, and foaming behaviors of polylactic acid in compressed CO2. *International Journal of Molecular Sciences*, *10(12)*, 5381-5397.